

Reviewer #2)

Baek and colleagues conducted a three-year investigation of multiple parameters of YRDW and elucidated how varying intrusions of YRDW influence heterotrophic prokaryote production and related effects. This study addresses an interesting topic and provides informative observational and laboratory data, which are clearly presented and support the authors' conclusions. While I believe the research contributes to the field of biogeochemistry and fits the scope of Biogeosciences, certain parts of the manuscript require further clarification and revision before publication.

**[Response]**

Thank you for your positive comments on our manuscript. We have revised the manuscript to improve its clarity and address the specific points raised in your comments below.

Comment #1) My main concern is that the study presents a large volume of data accompanied by some text that remains largely descriptive (somewhat lacks a line to easily follow), particularly in some of the Results section. I also recommend that the authors thoroughly revise the Abstract and Introduction to include a clear scientific question that establishes a logical narrative, making the study easier to follow and more engaging for readers.

Additionally, the authors could specify what constitutes refractory DOC (e.g., humic-like substances?), as this currently lacks a clear description in the Discussion and is somewhat obscured within the detailed information. Below, I also provide specific suggestions for revising the manuscript.

**[Response to comment #1]**

We appreciate this constructive comment. To reduce the descriptive nature of the Results section, and enhance clarity, we have added quantitative metrics (i.e., mean, range, p-values and correlations), created a new table (Table S1) and Figure (Fig. 3) to better illustrate seasonal and interannual patterns. We also toned down the Abstract for clarity and clarified the definition of refractory DOC in the Discussion.

**[Revised Results section (Section 3.2 – 3.3)]**

**3.2 DOC, Chl-*a* and primary production**

The vertical distributions of DOC reflected seasonal changes in water column structure (Fig. 3). In February and November, DOC concentrations were relatively homogeneous within the MLD (50–70 m), averaging  $65 \pm 2 \mu\text{M}$  ( $53 - 76 \mu\text{M}$ ) and  $64 \pm 2 \mu\text{M}$  ( $55 - 83 \mu\text{M}$ ), respectively (Fig. 3C, W). In contrast, during May and August, DOC concentrations increased with decreasing MLD, averaging  $72 \pm 1 \mu\text{M}$  ( $66 - 74 \mu\text{M}$ ) in May and  $86 \pm 3 \mu\text{M}$  ( $75 - 130 \mu\text{M}$ ) in August (Fig. 3K, Q; Table 1).

Elevated DOC concentrations were particularly evident in August within the low-salinity surface layer (upper 10 m), where values averaged  $95 \pm 19 \mu\text{M}$  ( $76-130 \mu\text{M}$ ; Fig. 3P, Q). Among the summer observations, August 2020 exhibited the highest DOC concentrations ( $104 \pm 5 \mu\text{M}$ ), which were significantly higher than those in August 2021 and 2022 ( $77 \pm 1 \mu\text{M}$  and  $80 \pm 3 \mu\text{M}$ , respectively;  $p = 0.002$ ), coinciding with the strongest influence of YRDW observed during the study period (Fig. 1C, 4A). Chl-*a* concentrations within the MLD followed a similar pattern: homogeneously low in February ( $0.47 \pm 0.02 \mu\text{g L}^{-1}$ ;  $0.42 - 0.49 \mu\text{g L}^{-1}$ ), increasing in May ( $1.05 \pm 0.24 \mu\text{g L}^{-1}$ ;  $0.77 - 1.22 \mu\text{g L}^{-1}$ ) with the development of thermal stratification, remaining elevated in August (avg.  $0.74 \pm 0.22 \mu\text{g L}^{-1}$ ;  $0.58 - 0.99 \mu\text{g L}^{-1}$ ) under strong haline stratification associated with YRDW intrusion, and decreased in November (avg.  $0.53 \pm 0.02 \mu\text{g L}^{-1}$ ;  $0.50 - 0.55 \mu\text{g L}^{-1}$ ) (Fig. 3I, P, L, R).

PP, integrated over the euphotic depth, followed a similar seasonal pattern, increasing from May to August and peaking at  $336 \pm 55 \text{ mg C m}^{-2} \text{ d}^{-1}$  (August 2021) and  $263 \pm 73 \text{ mg C m}^{-2} \text{ d}^{-1}$  (August 2022) (Fig. 4D). Notably, PP in August 2020 ( $182 \pm 77 \text{ mg C m}^{-2} \text{ d}^{-1}$ ) was significantly lower than other years ( $p = 0.028$ ) (Fig. 4D), despite high YRDW input.

### 3.3 Prokaryotes abundance and heterotrophic prokaryotes production

Mean PA within the euphotic depth was lowest and vertically homogeneous in February ( $0.46 \pm 0.03 \times 10^9 \text{ cells L}^{-1}$ ;  $0.35 - 0.59 \times 10^9 \text{ cells L}^{-1}$ ). In contrast, PA reached its highest values in May ( $1.28 \pm 0.09 \times 10^9 \text{ cells L}^{-1}$ ;  $0.48 - 1.88 \times 10^9 \text{ cells L}^{-1}$ ), before declining in August ( $0.99 \pm 0.09 \times 10^9 \text{ cells L}^{-1}$ ;  $0.37 - 2.36 \times 10^9 \text{ cells L}^{-1}$ ) and November ( $0.66 \pm 0.08 \times 10^9 \text{ cells L}^{-1}$ ;  $0.28 - 1.29 \times 10^9 \text{ cells L}^{-1}$ ) (Fig. 3; Table 1). PA correlated positively with DOC ( $\rho = 0.255$ ,  $p < 0.001$ ) and Chl-*a* ( $\rho = 0.281$ ,  $p < 0.001$ ). HPP within the euphotic depth followed a seasonal cycle: lowest in February ( $0.33 \pm 0.12 \mu\text{g C L}^{-1} \text{ d}^{-1}$ ;  $0.20 - 0.58 \mu\text{g C L}^{-1} \text{ d}^{-1}$ ), rising in May ( $3.73 \pm 1.37 \mu\text{g C L}^{-1} \text{ d}^{-1}$ ;  $1.76 - 5.86 \mu\text{g C L}^{-1} \text{ d}^{-1}$ ), reaching a

consistent summer peak in August ( $5.51 \pm 4.08 \mu\text{g C L}^{-1} \text{ d}^{-1}$ ;  $0.69 - 17.43 \mu\text{g C L}^{-1} \text{ d}^{-1}$ ), and then declining in November ( $0.83 \pm 0.26 \mu\text{g C L}^{-1} \text{ d}^{-1}$ ;  $0.43 - 1.24 \mu\text{g C L}^{-1} \text{ d}^{-1}$ ) (Fig. 4). HPP correlated positively with temperature ( $\rho = 0.525$ ,  $p < 0.001$ ), DOC ( $\rho = 0.457$ ,  $p < 0.001$ ) and Chl-*a* ( $\rho = 0.398$ ,  $p < 0.001$ )  
60 consistent with the observed summer peak.

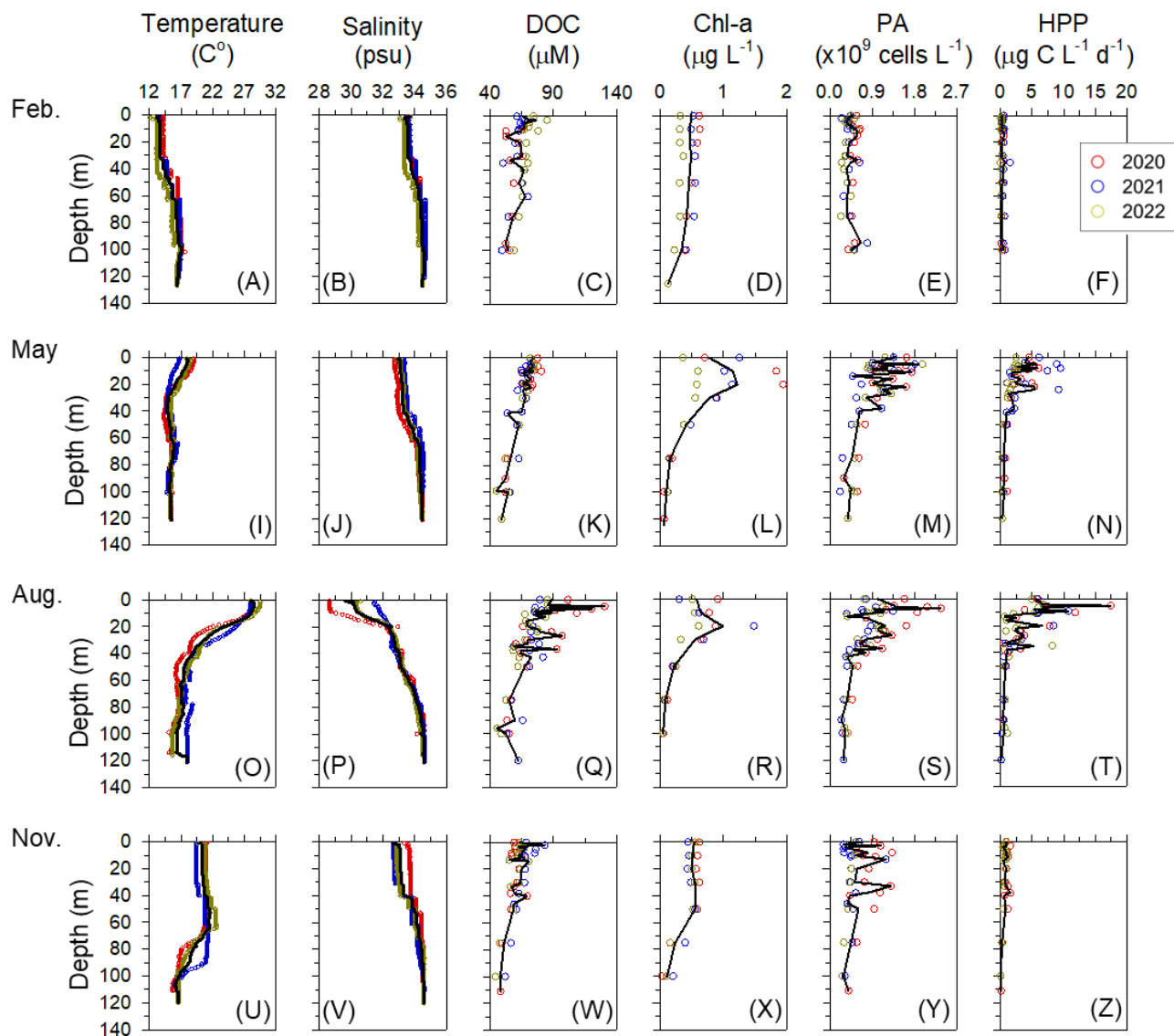


**Figure 3. Vertical profiles of temperature, salinity, dissolved organic carbon (DOC), chlorophyll-a (Chl-a), heterotrophic prokaryote abundance (PA), and heterotrophic prokaryote production (HPP) in the northern East China Sea from 2020 to 2022. Each symbol represents the average value at a given depth from 7–8 stations sampled during each survey, and the solid black line denotes the mean of the three-year averages.**

## [Revised Abstract]

Line 27: Accordingly, the enhanced HPP to primary production ratio ( $> 0.5$ ) in summer suggested enhanced carbon flow via microbial loop, which ultimately affects fishery structure and production by reducing energy efficiency in food web process.

→ Accordingly, the enhanced HPP-to-primary production ratio ( $> 0.5$ ) in summer may suggest enhanced carbon flow via microbial loop, potentially altering food-web structure and energy transfer efficiency.

Line 29: Our results demonstrating the contrasting impact of YRDW on regulating (i.e., either stimulating or suppressing) the HPP provide new insights into the microbial responses to climate change-induced large-scale freshwater discharge, which is applicable to other ocean basins receiving great freshwater inputs (e.g., Amazon River and Arctic Ocean) accompanied by increasing precipitation.

→ Our results, demonstrating that YRDW can either stimulate or suppress HPP, provide new insights into microbial responses to large-scale freshwater discharge, which may be relevant to systems influenced by substantial freshwater inputs (e.g., Amazon River and Arctic Ocean).

## [Revised Discussion]

Line 292: Accordingly, the humification index (HIX), used as a proxy for the refractory nature of DOM (Hansen et al., 2016; Li et al., 2019a), also reached its highest level ( $1.79 \pm 0.36$ ) in August 2020 (Fig. 6C). In environments where refractory organic matter is predominant, HP tend to utilize the organic matter more for cell maintenance (i.e., for energy-yielding respiration) rather than for biomass synthesis (i.e., production) (Carlson et al., 2007; Fasching et al., 2014).

→ Consistent with this, the HIX, proxy for the refractory nature of DOM (Hansen et al., 2016; Li et al., 2019a), also reached its highest level ( $1.79 \pm 0.36$ ) in August 2020 (Fig. 6C). HIX reflects the relative contribution of humic-like FDOM in the DOM pool, which is generally characterized by high aromaticity, molecular weight, and structural complexity (Hansen et al., 2016). Such humic-like FDOM are known to exhibit low biogeochemical reactivity and resistance to microbial

degradation, resulting in their persistence in aquatic environments (Yamashita and Tanoue, 2008; Cao et al., 2019). Under these conditions, HP tend to utilize organic matter primarily for cell maintenance (i.e., energy-yielding respiration) rather than for biomass synthesis (i.e., production) (Carlson et al., 2007; Fasching et al., 2014).

Line 31: climate change seems too ambitious to me.

**[Response]**

Thank you for this comment. We revised the sentence to remove the reference to climate change and to focus on the observed influence of large-scale freshwater discharge, as follows:

**[Revision]**

Line 31: Our results demonstrating the contrasting impact of YRDW on regulating (i.e., either stimulating or suppressing) the HPP provide new insights into the microbial responses to climate change-induced large-scale freshwater discharge

→ Our results demonstrating the contrasting impact of YRDW on regulating (i.e., either stimulating or suppressing) the HPP provide new insights into the microbial responses to ~~climate change-induced~~ large-scale freshwater discharge,

Line 116: pls specify 1% light penetration depth.

**[Response]**

Thank you for this comment. We have clarified that the 1% light penetration depth was defined as the euphotic depth, determined from Secchi disk measurements at each station, and is provided in the associated metadata (*Dataset\_Water\_column.csv*). Line 116 has been revised as follows:

**[Revision]**

Line 116: Seawater samples for chemical and biological analyses were collected at designated water depths of 0, 10, 20, 30, 50, 75, 100, 120 meters, as well as at the 1% light penetration depth.

→ Seawater samples for chemical and biological analyses were collected ~~concurrently at the same sampling stations. Sampling was conducted at standard depth~~ (0, 10, 20, 30, 50, 75, 100, and 120 m). ~~Samples for measuring PP were collected at depths corresponding to 30% and 1% of surface~~

photosynthetically active radiation (PAR), determined from Secchi disk measurements. The 1% light depth was defined as the euphotic depth (see *Dataset\_Water\_column.csv*). This sampling design enabled direct comparison of HPP and PP.

125

Line 117: how did you rinse the GFF filters? These suppose to be combusted to avoid potential carbon contamination.

**[Response]**

Yes, combusted GF/F filters are commonly recommended to minimize potential carbon contamination.

130 In this study, however, we used sterile syringe-type GF/F filters (0.7  $\mu\text{m}$  pore size, Whatman). Syringe-type filters have been used in previous dissolved organic matter (DOM) studies for sample preparation (Saadi et al., 2006; Nimptsch et al., 2014; Vonk et al., 2015).

Although combusted GF/F filters could also have been applied, syringe-type filters were selected in this study as a practical choice for field sampling involving multiple depths and stations. Prior to sample  
135 collection, each syringe-type filter was filtered with 90 mL of the corresponding seawater sample (three times the vial volume) to minimize potential contamination associated with filtration and handling. Such prewashing procedures can reduce potential contamination and DOM sorption during filtration (Halewood et al., 2022; Seo et al., 2025).

To further validate our DOC measurements, we compared our results with independent observations from  
140 a contemporaneous study. Han et al. (2023) reported elevated DOC concentrations associated with Changjiang diluted water (CDW=YRDW), with an average DOC concentration of  $102 \pm 7 \mu\text{M}$  during August 11–21, 2020, which closely overlaps with our sampling period (August 7–15, 2020; *Dataset\_Water\_column.csv*). These values are comparable to the DOC concentrations measured in this study ( $104 \pm 5 \mu\text{M}$ ), supporting the validity of our measurements.

145

Line 132: T-S, temperature-salinity?

**[Response]**

Thank you for this comment. We have clarified that T–S refers to temperature–salinity in line 132 in revised manuscript as follows:

150 **[Revision]**

Line 132: T–S diagram analysis was conducted using 1 m bin-averaged T–S data (Fig. 2).

→ ~~Temperature–salinity~~ (T–S) diagram analysis was conducted using 1 m bin-averaged T–S data (Fig. 2).

155 Line 153: pls also specify the depths.

**[Response]**

Thank you for this comment. Light penetration depths vary by season and among individual stations, making it impractical to specify all values directly in the manuscript. In response to your request to specify the light penetration depths, we have therefore uploaded a separate file  
160 (*Dataset\_Light\_penetration\_depth.csv*) to Zenodo. The manuscript was revised as follows:

**[Revision]**

Line 153: Water samples were obtained from six distinct photic depths, representing 100%, 50%, 30%, 12%, 5%, and 1% penetration of surface PAR, determined through the conversion of Secchi disc depth measurements at each sampling station.

165 → Water samples were obtained from six distinct photic depths, representing 100%, 50%, 30%, 12%, 5%, and 1% penetration of surface PAR, determined through the conversion of Secchi disc depth measurements at each sampling station (*see Dataset\_Light\_penetration\_depth.csv*).

Line 189: to be true, there are too many acronyms, I went back and forth for them, thus hard to follow the results. How about having an extra table to explain these acronyms?

170 **[Response]**

Thank you for this suggestion. We have added Table S3 as below, which summarizes all acronyms used in the manuscript to improve readability.

175



**Table S3. List of acronyms and abbreviations used in this study**

Acronym	Full term
CC	Chinese coastal current
DIN	Dissolved inorganic nitrogen
DIP	Dissolved inorganic phosphorus
DOC	Dissolved organic carbon
DOM	Dissolved organic matter
ECS	East China Sea
ES	East Sea
FDOM	Fluorescent dissolved organic matter
FDOM <sub>H</sub>	humic-like fluorescent dissolved organic matter
HIX	Humification index
HP	Heterotrophic prokaryotes
HPP	Heterotrophic prokaryotes production
KSW	Kuroshio source water
MLD	Mixed layer depth
nECS	northern East China Sea
NIFS	Korean national institute of fisheries science
PA	Heterotrophic prokaryotes abundance
PAR	Photosynthetically active radiation
SMW	Shelf mixed water
TWC	Taiwan warm current
TWW	Tsushima warm water
YRDW	Yangtze river diluted water
YS	Yellow Sea

Line 188-201: these are quite descriptive and lack a clear logical progression. I recommend revising this section to improve its flow and readability.

### [Response]

185 Thank you for this comment. We have revised Section 3.1 to improve clarity and logical flow by streamlining the text, clarifying the definitions of water masses, and relocating detailed temperature–salinity ranges to Table S1.

### [Revision]

#### 3.1 Hydrographic conditions

190 Based on Temperature-Salinity (T-S) diagrams, the current systems in the study area were defined by 2-4 water masses that vary seasonally (Fig. 2). The two main currents appearing in the nECS are the Kuroshio Source Water (KSW) and the Shelf Mixed Water (SMW) (Fig. 2). The KSW is formed by the convergence of the TWC and the TWW, which are both branches of the main Kuroshio Current in the nECS and are characterized by high temperature and salinity (Supplement Fig. S1). In contrast, the SMW  
195 is formed by the mixing of the KSW with the Chinese Coastal Current (CC). The CC, which is mainly observed on the shelf side of the East China Sea, is characterized by cold and low-salinity properties (Li et al., 2006). As a result, the SMW exhibits relatively lower temperature and salinity due to the influence of the CC. During February (winter), May (spring), and November (autumn), the nECS consisted of KSW and SMW (Fig. 2A, B, D, E, F, H, I, J, L; Table S1). However, during August (summer), a more complex  
200 water mass distribution was observed due to strong stratification and substantial freshwater input: TWC and YRDW were present near the surface, whereas TWW and SMW were observed in the mid to lower layers, which differed from other seasons (Fig. 2C, G, K; Table S1). The satellite images of sea surface salinity (Fig. 1), together with the T-S diagrams (Fig. 2), clearly revealed that YRDW ( $< 31$  psu, the blue-green colors in Fig. 1C, G, K) originating from the Yangtze River in August expands northeastward to  
205 the nECS located approximately 300 km away from the Yangtze River estuary. The expansion of YRDW to the nECS was greatest in August 2020, followed by August 2022 and 2021, respectively (Fig. 1; Fig. 2).

210 **Table S1. Seasonal temperature and salinity ranges used to define major water masses in the northern East China Sea in this study. KSW: Kuroshio source water, SMW: Shelf mixed water, YRDW: Yangtze river diluted water, TWW: Tsushima warm water, TWC: Taiwan warm current.**

	Seasonal temperature (°C) and salinity (psu) range				
	KSW	SMW	YRDW	TWW	TWC
Winter	8.4 < T < 24.5	8.8 < T < 15			
	33.6 < S < 35.2	32.4 < S < 33.6			
Spring	11.5 < T < 29.4	12 < T < 21			
	33.5 < S < 35.2	31.2 < S < 33.5			
Summer		14 < T < 23	23 < T	14 < T	23 < T
		31 < S < 34	S < 31	34 < S	31 < S < 34.2
Autumn	11.8 < T < 27.3	14.3 < T < 24.2			
	33.4 < S < 34.9	31.9 < S < 33.4			

Line 214: pls direct specify what are the extreme conditions.

**[Response]**

215 Thank you for this comment. Following your suggestion regarding Line 217, we considered that this sentence was more interpretative in nature and therefore better suited to the Discussion. As the reduced primary production observed in August 2020 under “extreme conditions” (i.e., high turbidity and nutrient imbalance) is already discussed in detail in Sections 4.2 (Line 296) and 4.3 (Line 341), we decided to remove this sentence. The revision is shown below:

220 **[Revision]**

Line 217: Notably, the PP in August 2020 ( $182 \pm 77 \text{ mg C m}^{-2} \text{ d}^{-1}$ ) was not stimulated compared to other years, despite the high YRDW input, suggesting a potential suppression of phytoplankton productivity under extreme YRDW conditions (Fig. 3D).

225 ➔ Notably, PP in August 2020 ( $182 \pm 77 \text{ mg C m}^{-2} \text{ d}^{-1}$ ) was significantly lower than other years ( $p = 0.028$ ) (Fig. 4D), despite high YRDW input.

Line 226: you already defined PA, pls check the entire MS for others.

**[Response]**

230 Thank you for this comment. We have checked the entire manuscript and ensured that all acronyms are  
defined consistently at their first occurrence.

235

240

245

250

- Cao, S., Sun, F., Lu, D., and Zhou, Y.: Characterization of the refractory dissolved organic matter (rDOM) in sludge alkaline fermentation liquid driven denitrification: effect of HRT on their fate and transformation, *Water Res.*, 159, 135–144, <https://doi.org/10.1016/j.watres.2019.04.063>, 2019.
- 260 Chiang, K.-P., Lin, C.-Y., Lee, C.-H., Shiah, F.-K., and Chang, J.: The coupling of oligotrich ciliate populations and hydrography in the East China Sea: spatial and temporal variations, *Deep-Sea Res. II*, 50, 1279–1293, [https://doi.org/10.1016/S0967-0645\(03\)00062-9](https://doi.org/10.1016/S0967-0645(03)00062-9), 2003.
- Ferguson, R. L., Buckley, E. N., and Palumbo, A. V.: Response of marine bacterioplankton to differential filtration and confinement, *Appl. Environ. Microbiol.*, 47, 49–55, [https://doi.org/10.1128/aem.47.1.49-](https://doi.org/10.1128/aem.47.1.49-55.1984)  
265 55.1984, 1984.
- Halewood, E., Opalk, K., Custals, L., Carey, M., Hansell, D. A., and Carlson, C. A.: Determination of dissolved organic carbon and total dissolved nitrogen in seawater using high temperature combustion analysis, *Front. Mar. Sci.*, 9, 1061646, <https://doi.org/10.3389/fmars.2022.1061646>, 2022.
- Han, H., Kim, H. B., Kim, J., Kim, G., Hwang, J., and Nam, S.: Dissolved organic matter in the  
270 northwestern Pacific marginal seas: insight into the distribution of its optical properties, *Front. Mar. Sci.*, 10, 1127803, <https://doi.org/10.3389/fmars.2023.1127803>, 2023.
- Hyun, J.-H. and Kim, K.-H.: Bacterial abundance and production during the unique spring phytoplankton bloom in the central Yellow Sea, *Mar. Ecol. Prog. Ser.*, 252, 77–88, <https://doi.org/10.3354/meps252077>, 2003.
- 275 Hyun, J.-H., Kim, S.-H., Yang, E. J., Choi, A., and Lee, S. H.: Biomass, production, and control of heterotrophic bacterioplankton during a late phytoplankton bloom in the Amundsen Sea Polynya, Antarctica, *Deep-Sea Res. Pt. II*, 123, 102–112, <https://doi.org/10.1016/j.dsr2.2015.10.001>, 2016.
- Hyun, J.-H.: Resource-limited heterotrophic prokaryote production and its potential environmental impact associated with Mn nodule exploitation in the northeast equatorial Pacific, *Microb. Ecol.*, 52, 244–  
280 252, <https://doi.org/10.1007/s00248-006-9012-5>, 2006.

- Kim, B., Baek, Y.-J., Han, H., Lee, H., Youn, S.-H., and Hyun, J.-H.: P-limited prokaryotic heterotrophic production and metabolic balance between prokaryotic carbon demand and phytoplankton primary production in summer in the central Yellow Sea, *Ocean Sci. J.*, 60, 14, <https://doi.org/10.1007/s12601-025-00209-x>, 2025.
- 285 Kirchman, D. L., Morán, X. A. G., and Ducklow, H.: Microbial growth in the polar oceans – role of temperature and potential impact of climate change, *Nat. Rev. Microbiol.*, 7, 451–459, <https://doi.org/10.1038/nrmicro2115>, 2009.
- Nimptsch, J., Woelfl, S., Kronvang, B., Giesecke, R., González, H. E., Caputo, L., Gelbrecht, J., von Tuempling, W., and Graeber, D.: Does filter type and pore size influence spectroscopic analysis of  
 290 freshwater chromophoric DOM composition?, *Limnologia*, 48, 57–64, <https://doi.org/10.1016/j.limno.2014.06.003>, 2014.
- Rahav, E., Raveh, O., Hazan, O., Gordon, N., Kress, N., Silverman, J., and Herut, B.: Impact of nutrient enrichment on productivity of coastal water along the SE Mediterranean shore of Israel – a bioassay approach, *Mar. Pollut. Bull.*, 127, 559–567, <https://doi.org/10.1016/j.marpolbul.2018.01.036>, 2018.
- 295 Robinson, C. and Williams, P. J. le B.: Temperature and Antarctic plankton community respiration, *J. Plankton Res.*, 15, 1035–1051, <https://doi.org/10.1093/plankt/15.9.1035>, 1993.
- Saadi, I., Borisover, M., Armon, R., and Laor, Y.: Monitoring of effluent DOM biodegradation using fluorescence, UV and DOC measurements, *Chemosphere*, 63, 530–539, <https://doi.org/10.1016/j.chemosphere.2005.07.075>, 2006.
- 300 Seo, J., Kim, G., Hwang, J., Na, T., Cho, H.-M., and Kim, J.: Measurement of fluorescent dissolved organic matter in water: methodological considerations and applications, *Biogeosciences*, 22, 4423–4431, <https://doi.org/10.5194/bg-22-4423-2025>, 2025.
- Tsai, A.-Y., Gong, G.-C., Huang, J.-K., and Lin, Y.-C.: Viral and nanoflagellate control of bacterial production in the East China Sea summer 2011, *Estuar. Coast. Shelf Sci.*, 120, 33–41,  
 305 <https://doi.org/10.1016/j.ecss.2013.01.006>, 2013.

Vonk, J. E., Tank, S. E., Mann, P. J., Spencer, R. G. M., Treat, C. C., Striegl, R. G., Abbott, B. W., and Wickland, K. P.: Biodegradability of dissolved organic carbon in permafrost soils and aquatic systems: a meta-analysis, *Biogeosciences*, 12, 6915–6930, <https://doi.org/10.5194/bg-12-6915-2015>, 2015.

White, P. A., Kalff, J., Rasmussen, J. B., and Gasol, J. M.: The effect of temperature and algal biomass  
310 on bacterial production and specific growth rate in freshwater and marine habitats, *Microb. Ecol.*, 21, 99–  
118, <https://doi.org/10.1007/BF02539147>, 1991.